Electronic Supplementary Material (ESI) for Journal of Materials Chemistry A.


# Supplementary Material

## Noble-metal-free $Ni_{10}MoCo_x$/Mo-Ni-O as an active and durable catalyst for hydrogen generation from hydrazine monohydrate

Si-Huan Qin, Yu-Ping Qiu*, Mu-Hua Chen, Ping Wang*

School of Materials Science and Engineering, South China University of Technology, Guangzhou 510641, P.R. China

*Corresponding author.

E-mails: msypqiu@scut.edu.cn (Y.P. Qiu), mspwang@scut.edu.cn (P. Wang)

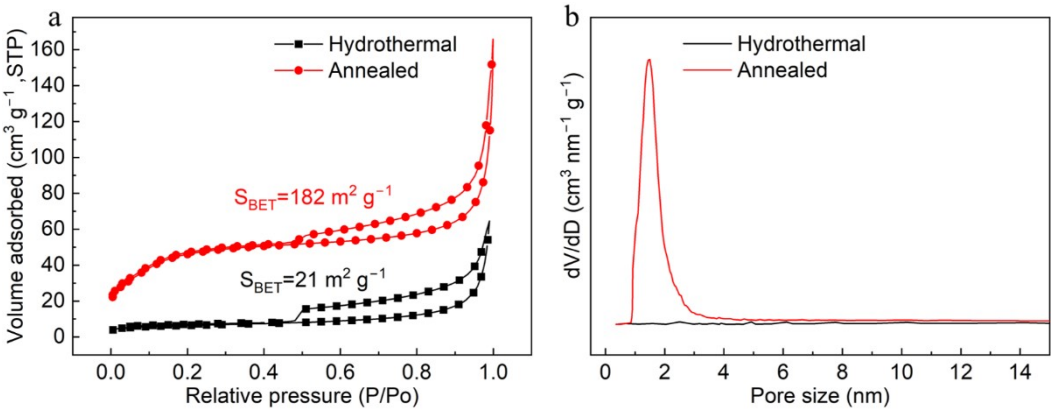


**Figure S1**. (a) $N_2$ adsorption-desorption isotherms and (b) pore size distributions of the hydrothermal and annealed samples.

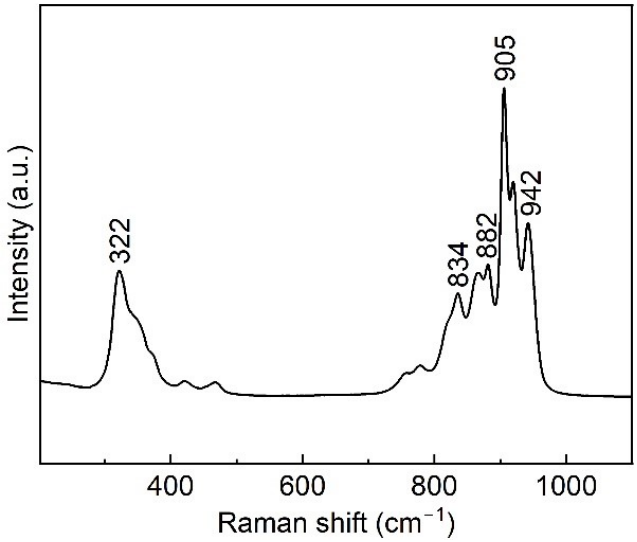


**Figure S2**. Raman spectrum of the hydrothermal sample.

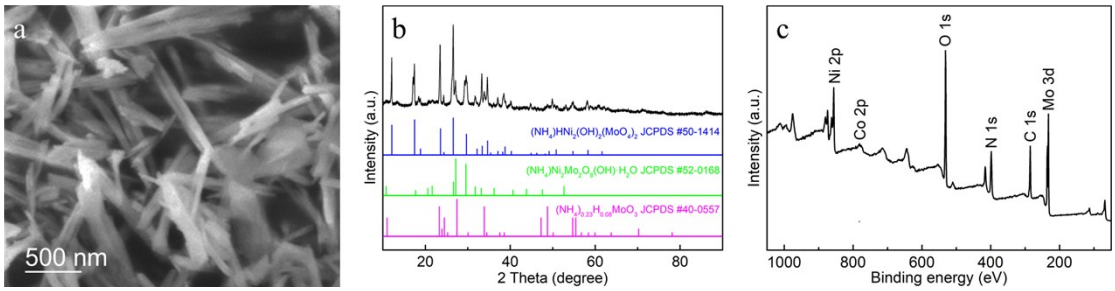


**Figure S3**. (a) FE-SEM image, (b) XRD pattern and (c) XPS spectrum of the SEA sample.

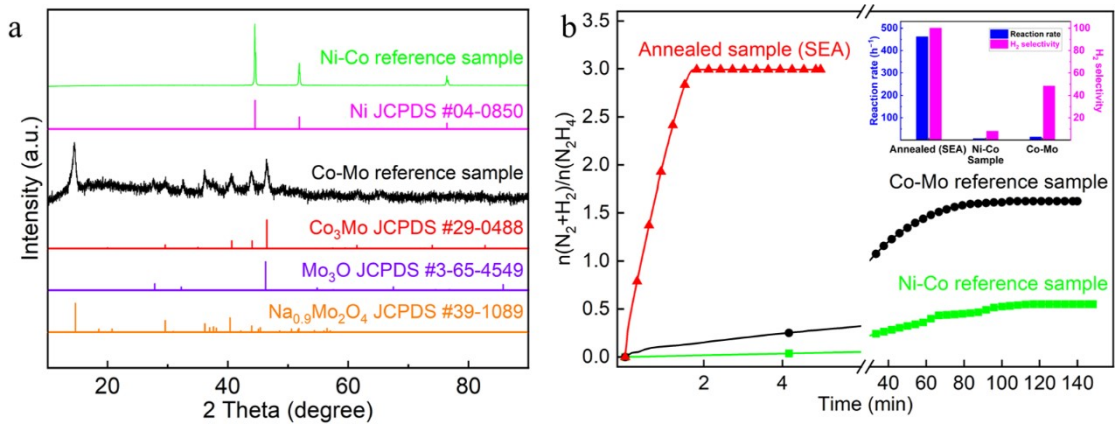


**Figure S4.** (a) XRD patterns of Ni-Co and Co-Mo reference samples. (b) Kinetic curves of $N_2H_4 \cdot H_2O$ decomposition over the annealed sample (SEA) and Ni-Co, Co-Mo reference samples. The inset shows the reaction rate and $H_2$ selectivity of the samples. The catalytic decomposition of $N_2H_4 \cdot H_2O$ was carried out in a 2 mL solution containing 0.5 M $N_2H_4 \cdot H_2O$ and 2.0 M NaOH at 70 °C, with metal/$N_2H_4$ ratio of 1:10.

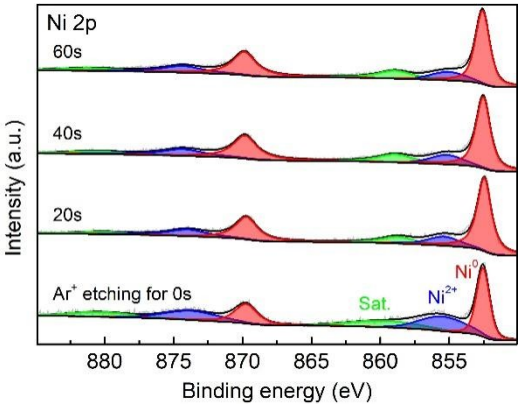


**Figure S5.** Ni 2p spectra of the annealed sample (SEA) as a function of etching time.

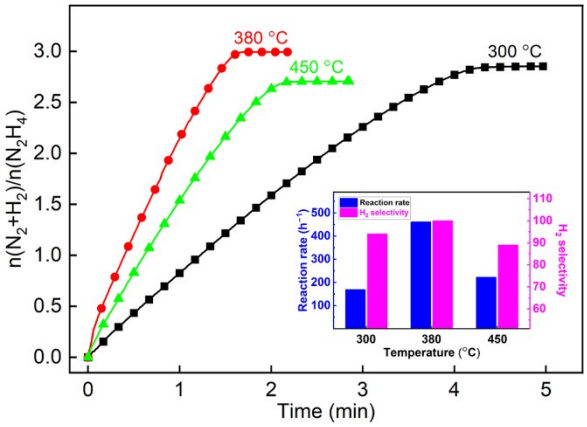


**Figure S6.** Kinetic curves of $N_2H_4 \cdot H_2O$ decomposition over the $Ni_{10}MoCo_x$/Mo-Ni-O catalyst annealed at different temperatures. The inset displays the reaction rate and $H_2$ selectivity as a function of annealing temperature. The catalytic decomposition of $N_2H_4 \cdot H_2O$ was carried out in a 2 mL solution containing 0.5 M $N_2H_4 \cdot H_2O$ and 2.0 M NaOH, with metal/$N_2H_4$ ratio of 1:10.

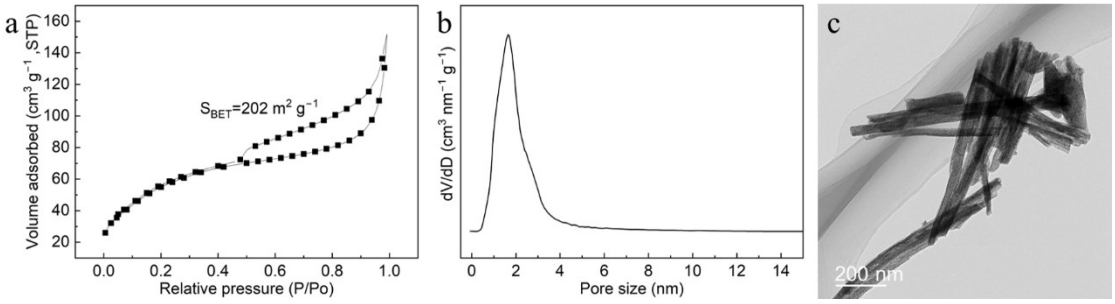


**Figure S7.** (a) $N_2$ adsorption-desorption isotherms, (b) pore size distributions and (c) TEM image of the $Ni_{10}Mo$/Mo-Ni-O catalyst.

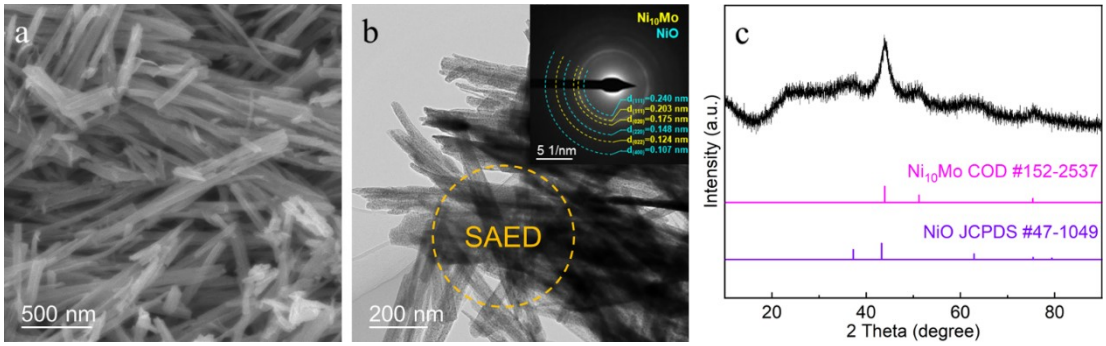


**Figure S8.** (a) FE-SEM image, (b) TEM image and the corresponding SAED pattern (inset) and (c) XRD pattern of the post-used $Ni_{10}MoCo_x$/Mo-Ni-O (SEA) sample.

**Table S1. A comparison of catalytic properties of $Ni_{10}MoCo_x$/Mo-Ni-O and relevant catalysts for $H_2$ generation from $N_2H_4 \cdot H_2O$.**

| Catalyst | Temperature (°C) | Reaction rate ($h^{-1}$) | $E_a$ (kJ $mol^{-1}$) | Reference |
|---|---|---|---|---|
| NiMoB-$La(OH)_3$ | 50 | 13.3 | / | 1 |
| $Ni_4W/WO_2/NiWO_4$ | 50 | 33 | / | 2 |
| $Ni/CeO_2$ | 50 | 34 | 56.2 | 3 |
| $Ni_{10}Mo$/Ni-Mo-O | 50 | 54.5 | 55.8 | 4 |
| Ni@TNTs | 60 | 96 | 53.2 | 5 |
| $Cu@Fe_5Ni_5$ | 70 | 11.9 | 79.2 | 6 |
| FeNi/Cu | 70 | 17.6 | 44 | 7 |
| $Ni_{0.9}Fe_{0.1}$-$Cr_2O_3$ | 70 | 82.2 | 86.3 | 8 |
| $CuNi/La_2O_2CO_3$/rGO | 70 | 114.3 | 65.5 | 9 |
| $Ni_3Fe$-$(CeO_x)_{0.15}$/rGO | 70 | 126.2 | 34.3 | 10 |
| $Ni_{10}MoCo_x$/Mo-Ni-O | 50<br>70 | 122<br>461 | 51.5 | This work |

**References**


1. J. Zhang, Q. Kang, Z. Yang, H. Dai, D. Zhuang, P. Wang, J. Mater. Chem. A, 2013, **1**, 11623−11628.
2. Q. Shi, D. X. Zhang, H. Yin, Y. P. Qiu, L. L. Zhou, C. Chen, H. Wu, P. Wang, ACS Sustainable Chem. Eng., 2020, **8**, 5595−5603.
3. W. Kang, A. Varma, Appl. Catal., B, 2018, **220**, 409−416.
4. Y. P. Qiu, G. X. Cao, H. Wen, Q. Shi, H. Dai, P. Wang, Int. J. Hydrogen Energy, 2019, **44**, 15110−15117.
5. H. Wang, L. Wu, A. Jia, X. Li, Z. Shi, M. Duan, Y. Wang, Chem. Eng. J., 2018, **332**, 637−646.
6. J. Wang, Y. Li, Y. Zhang, Adv. Funct. Mater., 2014, **24**, 7073−7077.
7. K. V. Manukyan, A. Cross, S. Rouvimov, J. Miller, A. S. Mukasyan, E. E. Wolf, Appl. Catal., A, 2014, **476**, 47−53.
8. J. Chen, H. Zou, Q. Yao, M. Luo, X. Li, Z. H. Lu, Appl. Surf. Sci., 2020, **501**, 144247.
9. X. Hong, Q. Yao, J. Long, X. Li, X. Chen, Z. H. Lu, Ind. Eng. Chem. Res., 2021, **60**, 16224−16232.
10. Y. Men, X. Du, G. Cheng, W. Luo, Int. J. Hydrogen Energy, 2017, **42**, 27165−27173.